The Astrophysical Journal, 616:638–642, 2004 November 20

HYDROGENATION OF CO ON PURE SOLID CO AND CO-H_2O MIXED ICE

Naoki Watanabe, Akihiro Nagaoka, Takahiro Shiraki, and Akira Kouchi
Institute of Low Temperature Science, Hokkaido University, N19-W8, Kita-ku, Sapporo, Hokkaido 060-0819, Japan;
watanabe@lowtem.hokudai.ac.jp
Received 2004 June 24; accepted 2004 July 29

ABSTRACT

Using a cold (30 K) atomic hydrogen beam, hydrogenation of CO on pure solid CO and CO-H_2O mixed ice is investigated at temperatures below 20 K. Hydrogenation proceeds efficiently on both pure solid CO and CO-H_2O mixed ice below 12 K, but the rate of reaction on pure CO decreases significantly at 15 K compared to CO-H_2O mixed ice. Hydrogenation of CO at 12 K and above is found to be promoted by H_2CO and H_2O molecules on the CO surface.

Subject headings: astrochemistry — dust, extinction — ISM: molecules — molecular processes

1. INTRODUCTION

Methanol (CH_3OH) and formaldehyde (H_2CO) have been identified in interstellar ice dusts at various abundances in association with high- and low-mass protostars (Dartois et al. 1999; Keane et al. 2001; Pontoppidan et al. 2003a). The observed solid-state abundances, however, cannot be achieved by the simple production of these molecules in gas phase followed by freezing onto dust (e.g., Shalabiea & Greenberg 1994). Therefore, it is generally believed that surface processes on the ice dust are necessary to produce the significant amounts of CH_3OH and H_2CO that have been observed.

Many theoretical studies have dealt with the hydrogenation of CO on interstellar dust as a key process in the production of H_2CO and CH_3OH as well as other energetic processes (e.g., Tielens & Whittet 1996; Charnley et al. 1997; Woon 2002). Using atomic hydrogen sprayed onto pure solid CO, Hiraoka et al. (1994) were the first to study the hydrogenation of CO experimentally, and recent revisiting of those experiments by the same group gave yields of less than 0.1% H_2CO (Hiraoka et al. 2002). As no CH_3OH product was detected, it was concluded that CH_3OH formation by the hydrogenation of CO is inefficient on icy grains. Our group has more recently shown experimentally that the hydrogenation of CO on H_2O ice is very efficient, producing both H_2CO and CH_3OH under the conditions of molecular clouds (Watanabe & Kouchi 2002; Watanabe et al. 2003; hereafter WSK03). This contradictory result has been attributed mainly to the very low fluence of hydrogen atoms in Hiraoka's experiments (Hidaka et al. 2004). Hidaka et al. (2004) described the differences between these experiments in detail, and suggested that the fluence of hydrogen atoms for 60 minutes of H spray in Hiraoka's experiments would be less than about 10^{15} atoms cm^{-2}, which is approximately 3 orders of magnitude smaller than that in WSK03. The fluence of 10^{15} atoms cm^{-2} is only less than that over 10^4 yr in the core of dense molecular clouds under the assumption that the number density of H is 1 cm^{-3} and the temperature is 10 K. In any case, the conclusion that CH_3OH formation by hydrogenation of CO is inefficient on icy grains is not convincing, because they have not measured the hydrogen flux and the fluence. However, the effect of surface composition on hydrogenation reactions remains open for discussion. Comparing the CO hydrogenation mechanism on H_2O with that on pure CO is important, as analysis of the observed solid-CO spectra indicates that CO would exist in apolar (probably CO) ice as well as H_2O ice (Teixeira et al. 1998; Pontoppidan et al. 2003b).

Using a cold atomic hydrogen beam, experiments were conducted in this study to examine CO hydrogenation on pure solid CO and CO-H_2O mixed ice at temperatures below 20 K.

2. EXPERIMENTAL

Two similar types of apparatuses were used in this study. The first one, Laboratory Setup for Surface Reactions in Interstellar Environment (LASSIE), was the setup used in the previous works (Watanabe & Kouchi 2002; WSK03; Hidaka et al. 2004). The second one, Apparatus for Surface Reaction in Astrophysics (ASURA), was newly designed and built based on the LASSIE. In the present experiment, measurements were performed by the ASURA if not otherwise specified. Details of the construction of the ASURA will be described elsewhere (N. Watanabe 2004, in preparation). Briefly, the ASURA consists of an atomic source chamber and a main chamber in which an aluminum substrate is mounted on the cold head of a He refrigerator (RDK-415, Sumitomo Heavy Industries). The temperature of the substrate is measured by a Si diode sensor with an accuracy of ± 0.2 K (DT470, LakeShore). The sample area is surrounded by a copper shroud that is connected to a liquid nitrogen reservoir to produce good H_2O pumping speed. The main chamber is evacuated using a turbomolecular pump (TG-900M, Osaka Vacuum; 900 liters s^{-1}), and the atomic source chamber is differentially pumped. The base pressure of the main chamber is approximately 5×10^{-10} torr, but reached 1×10^{-7} torr during beam operation.

The sample was produced by vapor deposition through a capillary plate on the substrate. For pure solid CO, a solid of about 10 monolayers (ML) in thickness was produced. As the surface structure of solid CO is not well known, the concept of a monolayer hereafter may differ from the usual idea of a closely packed layer. For CO-H_2O mixed ice, the samples were prepared in the same manner as in previous experiments (WSK03), producing a solid of about 30 ML in thickness with an H_2O/CO ratio of 4.

The design of the atomic source is almost the same as the LASSIE (Hidaka et al. 2004). Atomic hydrogen is produced by a microwave-induced plasma in a Pyrex tube and transferred

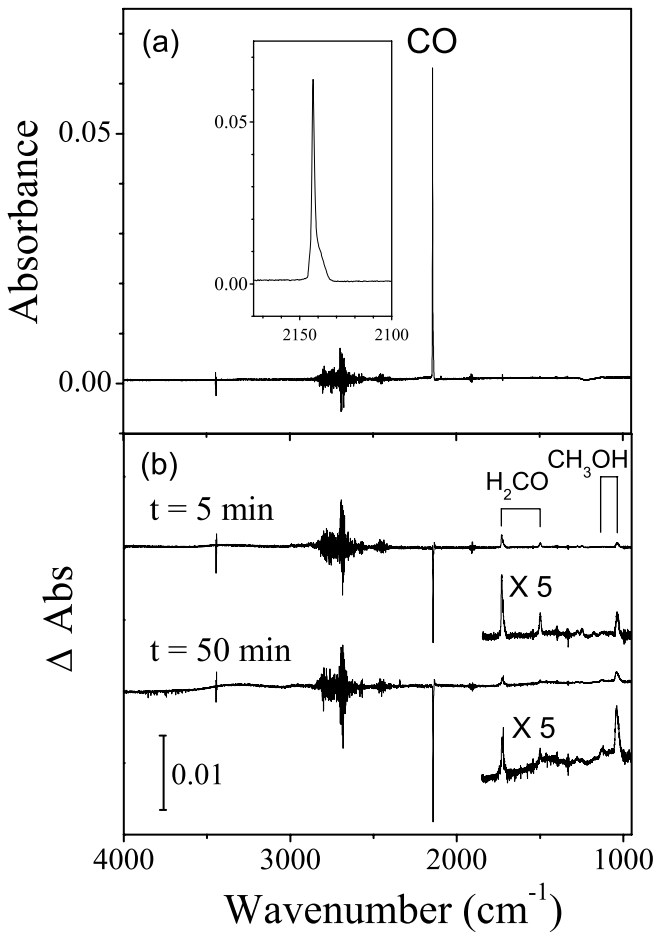

FIG. 1.—(*a*) Infrared absorption spectrum of initial (nonexposed) solid CO at 10 K, with a close-up of the CO peak in the region of 2175–2100 cm^{-1} inset. (*b*) Variation of infrared absorption spectra with exposure to H atoms. Spikes at 3445, 2915–2380, and 1903 cm^{-1} are due to noise caused by vibration of the He refrigerator.

via a series of polytetrafluoroethylene (PTFE) tubes to the target. A deflector is mounted at the end of the PTFE tube to eliminate charged particles and metastable H atoms that may escape from the plasma. Atoms can be cooled by another He refrigerator (V204SC5L, Daikin) connected to a copper tube that tightly sheaths the PTFE tube. The temperature of atoms can be controlled in a range above 20 K by a heater attached to the refrigerator. In the present experiments, the beam temperature was fixed at about 30 K. The dissociation fraction of H_2 and the H flux of the beam were measured by a quadrupole mass analyzer with a Faraday cup in front of the substrate as described previously (Watanabe & Kouchi 2002; Hidaka et al. 2004) and were estimated to be, respectively, 15% at least and 5×10^{14} cm^{-2} s^{-1}, about half that in previous experiments (WSK03). During exposure to H atoms, infrared absorption spectra of the target were measured by Fourier transform infrared (FTIR) spectroscopy with a resolution of 0.5 cm^{-1}.

3. RESULTS AND DISCUSSION

Figure 1 shows the infrared absorption spectrum of the initial pure solid CO and the variation in the spectra with exposure to H atoms at 10 K. The peak of the initial CO solid at 2142.5 cm^{-1} has a small shoulder at lower wavenumbers, attributable to a combination of the longitudinal optical (LO) mode at 2142.5 cm^{-1} and the transverse optical (TO) mode at 2138.5 cm^{-1} for crystalline CO (Chang et al. 1988). The resolution of FTIR spectroscopy was not sufficient to separate these peaks completely. Unfortunately, the spectra included a large amount of noise due to vibration of the closed-cycle He refrigerator. In Figure 1*b*, it is obvious that H_2CO and subsequently CH_3OH are produced as CO is consumed upon exposure to cold H atoms, representing the first clear evidence that CH_3OH is efficiently produced by the successive hydrogenation of CO and H_2CO even on pure solid CO. Although these hydrogenations were described as tunneling reactions previously (WSK03), further experiments are still required to obtain a conclusive result. The peaks are much sharper than those measured previously (Watanabe & Kouchi 2002; WSK03) because of the higher resolution of FTIR spectroscopy (0.5 cm^{-1} compared to 4 cm^{-1} previously). The spectra for CO-H_2O mixed ice are similar to those observed previously (WSK03) and are not shown here.

From the band areas in the spectra and the integrated band strengths reported, the column densities normalized to that of the initial CO are calculated and plotted for pure CO at 8, 10, 12, and 15 K and mixed ice at 8, 12, and 15 K as a function of exposure time in Figure 2. The integrated band strengths used are 1.1×10^{-17}, 9.6×10^{-18}, and 1.6×10^{-17} cm $molecule^{-1}$ for CO (2142 cm^{-1}; Jiang et al. 1975), H_2CO (1722 cm^{-1}; Schutte et al. 1993), and CH_3OH (1032 cm^{-1}; Kerkhof et al. 1999), respectively. Each data point is the average of three measurements. The sum of H_2CO and CH_3OH yields tends to be larger than CO consumption by factors of 1.2–1.7. This difference can be attributed to the ambiguity of integrated band strengths. The integrated band strengths would vary with the temperature and composition and would then be difficult to determine exactly. For example, the different integrated band strengths of CO in H_2O with a ratio of about 1/20 were reported to be 1.1×10^{-17} and 1.7×10^{-17} cm $molecule^{-1}$ by Gerakines et al. (1995) and Sandford et al. (1988), respectively. In the present experiments, the ice component consists of more than three species. For pure solid CO, the conversion rates of CO to H_2CO at 8 K, as indicated by the slopes of the CO and H_2CO plots at the beginning of H exposure, are close to that at 10 K. However, the rate of H_2CO conversion to CH_3OH at 8 K is lower than that at 10 K, as indicated by decrease in H_2CO after 7 minutes of exposure. The mixed-ice measurements at 8–15 K (Fig. 2, *right*) give similar results and are also consistent with previous measurements (WSK03). The temperature dependence of pure CO differs significantly from that of the mixed ice at 12 K and above. In the case of CO-H_2O mixed ice, the successive hydrogenation proceeds efficiently at temperatures higher than about 15 K, but slow again at 20 K possibly because of a drop in the sticking probability of H atoms to the H_2O ice. For pure CO, the reaction rates become much slower at 12 K, and fall drastically at 15 K. These differences in the temperature dependence of reactions are attributable to the different sticking probability of H atoms. It is reasonable to expect that the sticking probability of H atoms to hydrogen-bonded H_2O ice is larger than that to the van der Waals–bonded CO solid. Although the sticking probability for solid CO has not been reported, it appears, based on the present results, that it may decrease significantly at around 15 K, above which hydrogenation is virtually halted. For the mixed ice, it appears that H atoms stick to H_2O initially and then react with adjacent CO molecules even at 15 K.

It is worth noting that CO decay in the solid CO at 12 K does not follow a single exponential at the beginning of H exposure, whereas CO decay in the mixed ice can be fitted fairly well by a

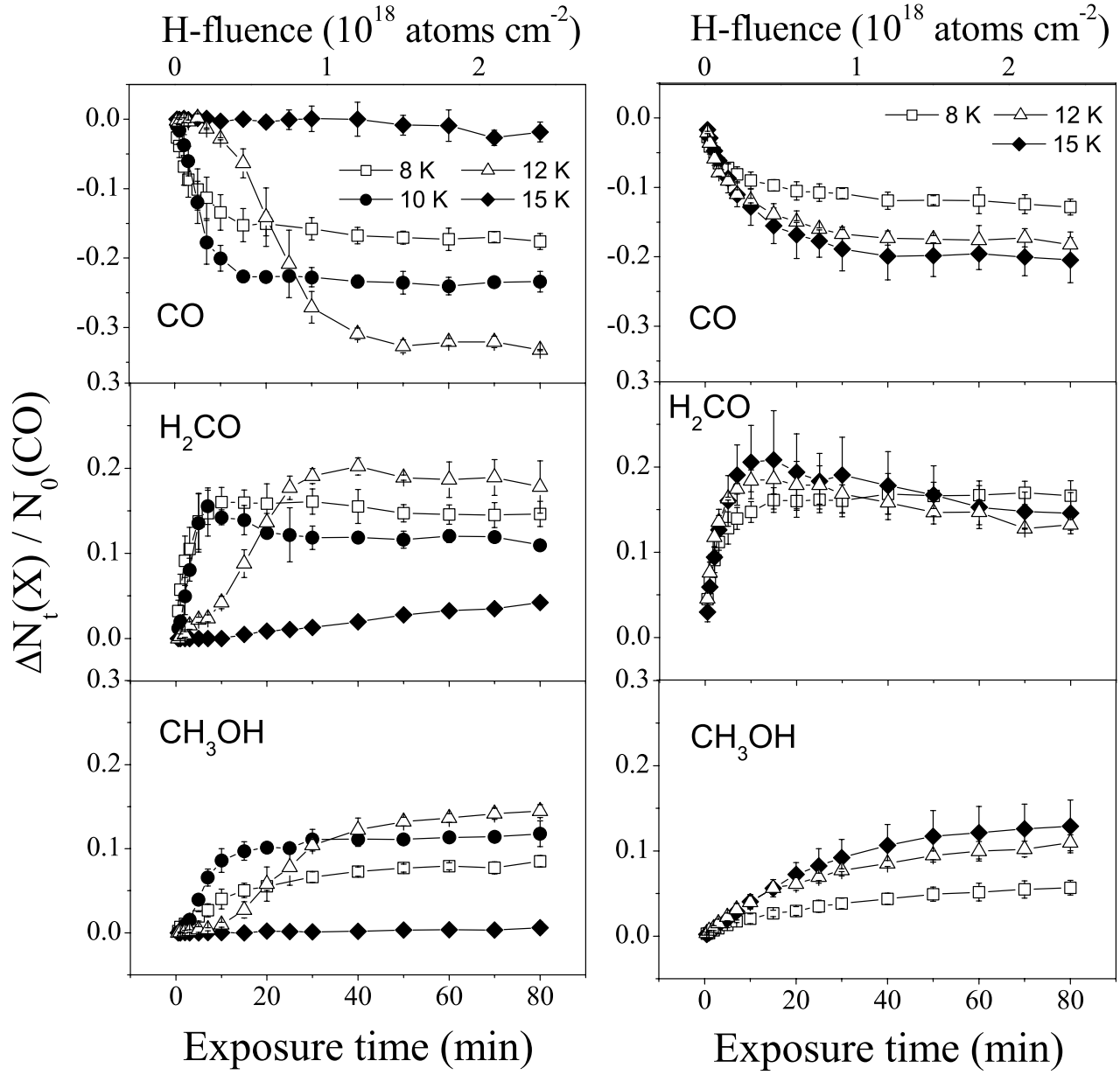

FIG. 2.—Variation in column densities for pure solid CO (*left*) and CO-H_2O mixed ice (*right*) with H exposure time. Column densities are normalized to initial CO. Error bars represent statistical error.

single exponential even at 20 K, where the decay is very slow (Awad et al. 2004). The non–single-exponential behavior may be governed by the change in sticking probability during H exposure, where the sticking of H atoms on pure CO and subsequent hydrogenation would be very inefficient at the beginning of exposure at 12 K. However, once H_2CO molecules are produced on the surface, H adsorption and hydrogenation will be enhanced. H_2CO may start to work catalytically after approximately 10 minutes of exposure, where the slope of CO decrease becomes steep (see Fig. 2, *left*). The H_2CO molecules are produced by about 3% of the initial amount of CO over 10 minutes. As discussed below, the hydrogenation proceeds only within the first several ML. When the H_2CO yield of 3% relative to the total solid CO (10 ML) accumulates near the surface, it corresponds to the coverage of 30% at the surface. To confirm this process, a pure solid CO sample covered with about 0.3 ML of H_2CO was exposed to H atoms at 12 K using the LASSIE with approximately twice the H flux of the ASURA. The CO decay for the H_2CO-covered CO is plotted against that for pure CO in Figure 3. The H_2CO coverage clearly enhances the hydrogenation of CO at the beginning of exposure (<10 minutes), but the total CO loss after 30 minutes is greater for the pure CO, probably also because of the coverage effect, which prevents buried CO molecules from reacting. The shape of the CO decay curve at 12 K therefore appears to be determined by the surface density of H_2CO molecules, indicating that the sticking probability of H atoms to H_2CO is larger than to CO. This is also supported by fitting using a simple rate equation. Assuming that the sticking probability (H_2CO yield) P_t increases in proportion to exposure time t in the early stage of exposure, the rate of CO loss can be expressed by

$$\frac{d[\Delta\mathrm{CO}]_t}{dt} = -P_t f k([\mathrm{CO}]_0 - [\Delta\mathrm{CO}]_t), \qquad (1)$$

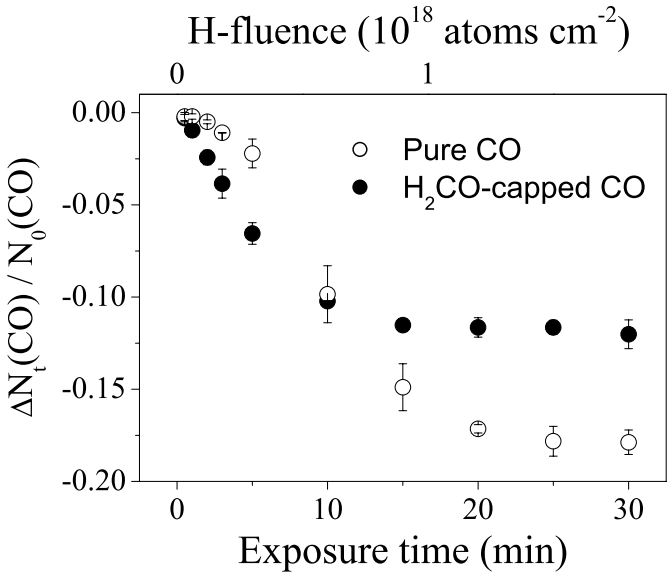

FIG. 3.—Variation in column densities for CO at 12 K on pure solid CO and CO covered with 0.3 ML of H_2CO. The data were obtained by experiments using the LASSIE.

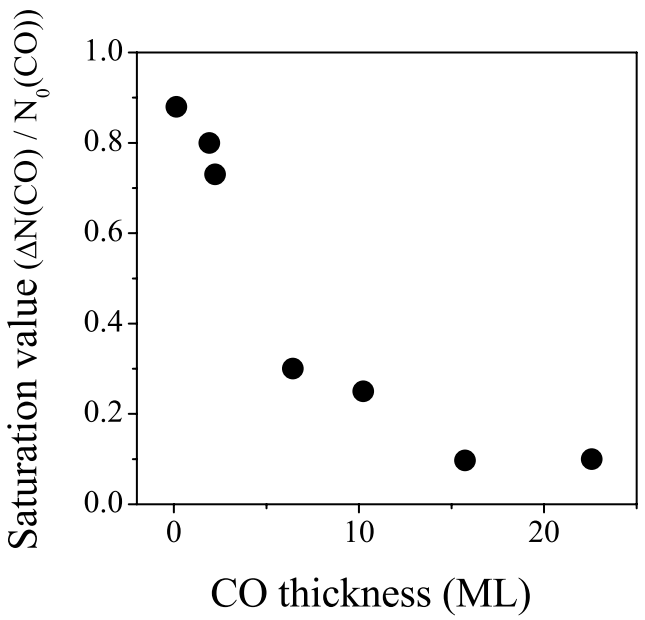

FIG. 4.—Dependence of saturation value of CO loss on thickness of initial solid CO at 12 K.

where $P_t \propto t$, k (cm^2) is the effective cross section of the reaction, and f is the H flux. Solving equation (1) gives

$$[\Delta CO]_t \propto e^{-\alpha k f t^2} - 1, \quad (2)$$

where $\alpha = P_t/t$. Equation (2) reproduces the initial behavior of CO loss at 12 K very well.

In Figure 2 (*left*), the CO losses become saturated after long exposures at 8–12 K. This type of saturation was also found previously for the mixed ice (WSK03). The saturation is related not to balance between hydrogenation (forward) and H abstraction (reverse) processes, but to the diffusion length of H in solid CO. The dependence of the saturation value on the initial thickness of pure solid CO at 12 K measured by the LASSIE is shown in Figure 4. At an initial thickness of less than 5 ML, more than 70% of the CO is eventually consumed, indicating that the reverse process is minor relative to the forward process and that CO hydrogenation occurs within only several ML of the surface. The saturation value increases with the temperature of the CO, implying that the diffusion length of H in CO increases with temperature. As shown in Figure 2 (*left*), with an initial CO thickness of 10 ML in the present study, only about 1.7, 2.4, and 3.3 ML of the surface molecules reacted at 8, 10, and 12 K, respectively. The saturation values at the same temperatures, representing the diffusion length of H atoms, are larger for solid CO than for the mixed ice (Fig. 2, *right*), assuming that the CO is distributed uniformly in the H_2O ice.

The conversion of H_2CO to CH_3OH also saturates at long exposure times. As the reverse process from CH_3OH to H_2CO by H atoms is minor (Hidaka et al. 2004), this saturation cannot be due to a balance of the forward and reverse processes. It therefore appears that the H diffusion length, which is dependent on the composition, is responsible for the saturation. Hidaka et al. (2004) exposed H_2CO solid with an initial thickness of 8 ML to H atoms and found that only 17% (equivalent to 1.4 ML) of the initial H_2CO was finally converted to CH_3OH at 15 K. It is therefore expected that the diffusion length of H atoms in H_2CO is shorter than 1.4 ML at 12 K. As the diffusion length in CO is about 3.3 ML at 12 K, the total CH_3OH yield from H_2CO tends to be smaller than that for H_2CO from CO at long exposure times. The structure of the molecular layers may thus be onion-like, with CH_3OH molecules at the top, H_2CO molecules in the middle, and CO at the bottom. This concept is similar to that of the three-phase model proposed by Hasegawa & Herbst (1993).

4. ASTROPHYSICAL IMPLICATION

It has been recognized that CO molecules are embedded in various types of ices (for a review, see Boogert & Ehrenfreund 2004). The results of the present study on the hydrogenation of CO in pure solid CO and H_2O ice clearly indicate that H_2CO and CH_3OH are produced by the hydrogenation of CO even in pure solid CO under the conditions of molecular clouds. It was also demonstrated that the surface composition and temperature affect the hydrogenation of CO. At below 12 K, the hydrogenation of CO proceeds efficiently both in pure solid CO and H_2O ice; between 12 and 15 K, the formation of H_2CO and CH_3OH is most efficient for CO in H_2O ice but is markedly suppressed in pure solid CO; and above 20 K, CO hydrogenation is very slow in H_2O ice and almost halted in pure solid CO. Within the framework of the surface reactions, this temperature dependence suggests that pure solid CO on dust undergoes very little evolution if the temperature of the cloud is above 15 K but below the evaporation temperature of solid CO. Ceccarelli et al. (2001) claimed that the hydrogenation of CO in H_2O is significantly more efficient than that in apolar CO ice. The present results qualitatively support their argument. Once H_2CO is produced on solid CO, CO hydrogenation is enhanced at 12 K because of an increase in the H sticking probability. It has been shown previously that the hydrogenation of H_2CO in solid H_2CO proceeds significantly even at 20 K, at which temperature the hydrogenation of CO in H_2O is very slow, although the hydrogenation of H_2CO is slower than that of CO (Hidaka et al. 2004). This implies that H_2CO acts as a better catalyst than H_2O. It is interesting that the presence of H_2CO is responsible not only for the formation of CH_3OH but also for

the hydrogenation of CO. Even in molecular clouds above 12 K, if H_2CO is produced on solid CO by another process such as photolysis, CO hydrogenation may be activated. Thus, H_2CO and CH_3OH can be produced by hydrogenation of CO in pure solid CO, but the reactions depend strongly on the dust temperature and the composition of the surface. Appropriate conditions are therefore crucial for the evolution of CO by hydrogenation.

Assuming a hydrogen number density of 1 cm^{-3}, the hydrogen fluences in a 10 K molecular cloud, where the gas temperature is the same as that of the dust, will be 1.3×10^{16}, 1.3×10^{17}, and 1.3×10^{18} cm^{-2} over 10^4, 10^5, and 10^6 yr. In the present experiment, these fluences approximately correspond to exposure times of 1, 4, and 40 minutes at 10 K. The fluences at 12 K can be similarly calculated. The ratios of column densities, CO/CH_3OH and H_2CO/CH_3OH, for each fluence are plotted against the results of the previous experiments (WSK03) and observations in Figure 5. The plots for the experimental results vary from the right to the left with the increase of H fluence. The leftmost plots correspond to 10^6 yr. The present results for the H fluence equivalent to that over 10^6 yr in molecular clouds reproduce the observations fairly well. For pure CO, the data at 12 K are closest to the observations, while the 15 K results are closest for the mixed ice. For both, thinner ices produce higher abundances of CH_3OH relative to CO and H_2CO. The experimental conditions for thinner ice may simulate higher H/CO ratios of accretion. The ratio of H_2CO/CH_3OH for pure CO tends to be larger than that for the mixed ice at the lower ratio of CO/CH_3OH, and this tendency becomes stronger for thinner ices. This feature can be explained by onion-like structure, as described above. When CO molecules are deposited on the surface, the CO molecules can readily aggregate into a bulk even below 1 ML coverage. Once H_2CO layers have been produced on the solid CO, only the upper layer of the H_2CO can be converted to CH_3OH, resulting in significant fraction of remnant H_2CO. In the case of the mixed ice (WSK03), isolated CO is abundant in H_2O and is available for the formation of CH_3OH.

As the probability of H-H recombination is proportional to the square of the surface coverage, the fraction of H atoms consumed by recombination becomes smaller under the conditions of low H flux in molecular clouds. Thus, in molecular clouds, the ratios of CO/CH_3OH and H_2CO/CH_3OH tend to be smaller than those in the experiments.

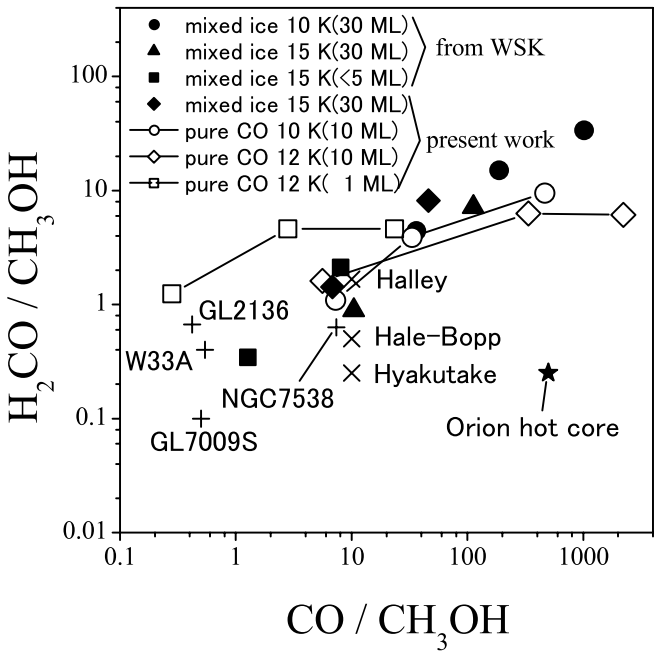

FIG. 5.—Column density ratios of H_2CO and CO relative to CH_3OH in comparison with results for mixed ice (WSK03) and observations. Open symbols represent results for pure solid CO, and solid symbols indicate mixed-ice results. Previous results are denoted by WSK on the legend. Results for 1 ML of pure solid CO were obtained with the LASSIE. Plots vary from right to left with the increase of H fluence. Leftmost plots correspond to 10^6 yr. Observations are denoted by plus signs for interstellar ice (Keane et al. 2001), crosses for comets, and a star for the Orion hot core (Ehrenfreund & Charnley 2000).

This work was supported in part by a Grant-in-Aid for Scientific Research from the Japan Society for the Promotion of Science.

REFERENCES

Awad, Z., Chigai, T., Kimura, Y., Shalabiea, O. M., & Yamamoto, T. 2004, ApJ, submitted
Boogert, A. C. A., & Ehrenfreund, P. 2004, in ASP Conf. Ser. 309, Astrophysics of Dust, ed. A. N. Witt, G. C. Clayton, & B. T. Draine (San Francisco: ASP), 547
Ceccarelli, C., Loinard, L., Castets, A., Tielens, A. G. G. M., Caux, E., Lefloch, B., & Vastel, C. 2001, A&A, 372, 998
Chang, H. C., Richardson, H. H., & Ewing, G. E. 1988, J. Chem. Phys., 89, 7561
Charnley, S. B., Tielens, A. G. G. M., & Rodgers, S. D. 1997, ApJ, 482, L203
Dartois, E., Schutte, W. A., Geballe, T. R., Demyk, K., Ehrenfreund, P., & d'Hendecourt, L. 1999, A&A, 342, L32
Ehrenfreund, P., & Charnley, S. B. 2000, ARA&A, 38, 427
Gerakines, P. A., Schutte, W. A., Greenberg, J. M., & van Dishoeck, E. F. 1995, A&A, 296, 810
Hasegawa, I. T., & Herbst, E. 1993, MNRAS, 263, 589
Hidaka, H., Watanabe, N., Shiraki, T., Nagaoaka, A., & Kouchi, A. 2004, ApJ, 614, 1124
Hiraoka, K., Ohashi, N., Kihara, Y., Yamamoto, K., Sato, T., & Yamashita, A. 1994, Chem. Phys. Lett., 229, 408
Hiraoka, K., Sato, T., Sato, S., Sogoshi, N., Yokoyama, T., Takashima, H., & Kitagawa, S. 2002, ApJ, 577, 265
Jiang, G. J., Person, W. B., & Brown, K. G. 1975, J. Chem. Phys., 62, 1201
Keane, J. V., Tielens, A. G. G. M., Boogert, A. C. A, Schutte, W. A., & Whittet, D. C. M. 2001, A&A, 376, 254
Kerkhof, O., Schutte, W. A., & Ehrenfreund, P. 1999, A&A, 346, 990
Pontoppidan, K. M., Dartois, E., van Dishoeck, E. F., Thi, W.-F., & d'Hendecourt, L. 2003a, A&A, 404, L17
Pontoppidan, K. M., et al. 2003b, A&A, 408, 981
Sandford, S. A., Allamandola, L. J., Tielens, A. G. G. M., & Valero, G. J. 1988, ApJ, 329, 498
Schutte, W. A., Allamandola, L. J., & Sandford, S. A. 1993, Icarus, 104, 118
Shalabiea, O. M., & Greenberg, J. M. 1994, A&A, 290, 266
Teixeira, T. C., Emerson, J. P., & Palumbo, M. E. 1998, A&A, 330, 711
Tielens, A. G. G. M., & Whittet, D. C. B. 1996, in IAU Symp. 178, Molecules in Astrophysics: Probes & Processes, ed. E. F. van Dishoeck (Dordrecht: Kluwer), 45
Watanabe, N., & Kouchi, A. 2002, ApJ, 571, L173
Watanabe, N., Shiraki, T., & Kouchi, A. 2003, ApJ, 588, L121 (WSK03)
Woon, D. 2002, ApJ, 569, 541